

AD-A056 384

LOCKHEED MISSILES AND SPACE CO INC PALO ALTO CALIF PA--ETC F/G 8/7
DOUBLY ASYMPTOTIC, BOUNDARY-ELEMENT ANALYSIS OF DYNAMIC SOIL-ST--ETC(U)
MAR 78 P G UNDERWOOD, T L GEERS

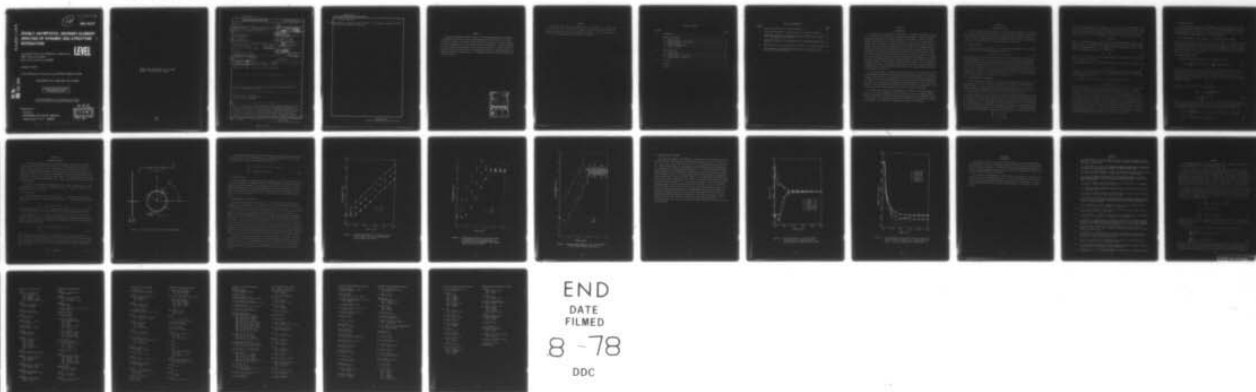
UNCLASSIFIED

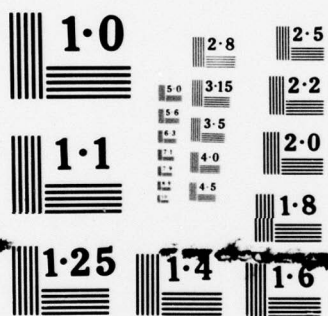
LMSC/D624828

DNA-4512T

NL

OF
ADA
066384





NATIONAL BUREAU OF STANDARDS
MICROCOPY RESOLUTION TEST CHART

AD A 056384

(12)

AD-E300 274

DNA 4512T

DOUBLY ASYMPTOTIC, BOUNDARY-ELEMENT ANALYSIS OF DYNAMIC SOIL-STRUCTURE INTERACTION

LEVEL II

Lockheed Palo Alto Research Laboratory
3251 Hanover Street
Palo Alto, California 94304

31 March 1978

Topical Report for Period 1 June 1975—31 March 1978

CONTRACT No. DNA 001-75-C-0294

APPROVED FOR PUBLIC RELEASE;
DISTRIBUTION UNLIMITED.

THIS WORK SPONSORED BY THE DEFENSE NUCLEAR AGENCY
UNDER RDT&E RMSS CODE B344075464 Y99QAXSC06137 H2590D.

Prepared for
Director
DEFENSE NUCLEAR AGENCY
Washington, D. C. 20305

DDC
RECEIVED
JUL 20 1978
B

78 06 26 010

AD No. _____
DDC FILE COPY

Destroy this report when it is no longer
needed. Do not return to sender.



UNCLASSIFIED

SECURITY CLASSIFICATION OF THIS PAGE (When Data Entered)

REPORT DOCUMENTATION PAGE		READ INSTRUCTIONS BEFORE COMPLETING FORM
1. REPORT NUMBER DNA 4512T	2. GOVT ACCESSION NO.	3. RECIPIENT'S CATALOG NUMBER
4. TITLE (and Subtitle) DOUBLY ASYMPTOTIC, BOUNDARY-ELEMENT ANALYSIS OF DYNAMIC SOIL-STRUCTURE INTERACTION.		5. TYPE OF REPORT & PERIOD COVERED Topical Report, for Period 1 June 1975—31 March 1978
7. AUTHOR(s) P. G. Underwood T. L. Geers		6. PERFORMING ORG. REPORT NUMBER LMSC/D624828
9. PERFORMING ORGANIZATION NAME AND ADDRESS Lockheed Palo Alto Research Laboratory 3251 Hanover Street Palo Alto, California 94304		8. CONTRACT OR GRANT NUMBER(s) DNA 001-75-C-0294
11. CONTROLLING OFFICE NAME AND ADDRESS Director Defense Nuclear Agency Washington, D.C. 20305		10. PROGRAM ELEMENT, PROJECT, TASK AREA & WORK UNIT NUMBERS Subtask Y99QAXSC061-37
13. MONITORING AGENCY NAME & ADDRESS (if different from Controlling Office) DNA, SBIE		12. REPORT DATE 31 March 1978
15. DISTRIBUTION STATEMENT (of this Report) 4512T, AD-E300 274		13. NUMBER OF PAGES 32
17. DISTRIBUTION STATEMENT (of the abstract entered in Block 20, if different from Report)		15. SECURITY CLASS (of this report) UNCLASSIFIED
18. SUPPLEMENTARY NOTES This work sponsored by the Defense Nuclear Agency under RDT&E RMSS Code B344075464 Y99QAXSC06137 H2590D.		15a. DECLASSIFICATION DOWNGRADING SCHEDULE
19. KEY WORDS (Continue on reverse side if necessary and identify by block number) Soil-Structure Interaction Doubly Asymptotic Approximations Boundary Element Techniques		
20. ABSTRACT (Continue on reverse side if necessary and identify by block number) This report describes a doubly asymptotic (DA), boundary-element (BE) treat- ment of a surrounding soil medium that offers considerable promise for dynamic soil-structure interaction analysis. The soil-structure interaction is reduced to a surface relationship that is asymptotically exact at both high and low frequencies. Governing equations for linear problems are developed in matrix form for application to complex structures. Numerical results are presented for a two-dimensional problem for which analytical		

DD FORM 1 JAN 73 1473

EDITION OF 1 NOV 65 IS OBSOLETE

UNCLASSIFIED

SECURITY CLASSIFICATION OF THIS PAGE (When Data Entered)

78 06 26 010
2/0118

CONT

cl

UNCLASSIFIED

SECURITY CLASSIFICATION OF THIS PAGE(When Data Entered)

20. ABSTRACT (Continued)

Cont solutions have appeared in the literature. Good agreement between the DA/BE and analytical results is observed.

UNCLASSIFIED

SECURITY CLASSIFICATION OF THIS PAGE(When Data Entered)

SUMMARY

This report describes a doubly-asymptotic (DA), boundary-element (BE) treatment of a surrounding soil medium that offers considerable promise for dynamic soil-structure interaction analysis. The soil-structure interaction is reduced to a surface relationship that is asymptotically exact at both high and low frequencies. Governing equations for linear problems are developed in matrix form for application to complex structures. Numerical results are presented for a two-dimensional problem for which analytical solutions have appeared in the literature. Good agreement between the DA/BE and analytical results is observed.

ACCESSION for		
NTIS	Write Section	<input checked="" type="checkbox"/>
DDC	Book Section	<input type="checkbox"/>
UNANNOUNCED		<input type="checkbox"/>
JUSTIFICATION		
BY		
DISTRIBUTION/AVAILABILITY CODES		
Dist.	Avail. and/or	SPECIAL
A		

PREFACE

The authors express their appreciation to Drs. J. A. DeRuntz, C. A. Felippa, and K. C. Park, and to Mr. E. M. Olsen, for valuable consultation on the intricacies of boundary integral equations and their numerical solution. A debt is also owed to Dr. C.-L. Yen for providing important analytical check results.

TABLE OF CONTENTS

<u>Section</u>		<u>Page</u>
I	INTRODUCTION - - - - -	5
II	GOVERNING EQUATIONS - - - - -	6
	2.1 STRUCTURAL MODEL - - - - -	6
	2.2 DOUBLY ASYMPTOTIC APPROXIMATION - - - - -	6
	2.3 RESPONSE EQUATION - - - - -	8
	2.4 MEDIUM STIFFNESS MATRIX - - - - -	8
	2.5 SOLUTION PROCEDURE - - - - -	9
III	NUMERICAL RESULTS - - - - -	11
	3.1 INCIDENT WAVE - - - - -	11
	3.2 CIRCULAR CAVITY - - - - -	13
	3.3 CONCRETE SHELL IN SLOW GRANITE - - - - -	13
	3.4 CONCRETE SHELL IN GRANITE - - - - -	17
IV	CONCLUSION - - - - -	20
	REFERENCES - - - - -	21
	APPENDIX - - - - -	23

LIST OF ILLUSTRATIONS

<u>Figure</u>		<u>Page</u>
1	Geometry and Notation for the Check Problems - - - - -	12
2	Displacement Response of a Circular Cavity to an Incident Step-wave - -	14
3	Displacement Response of a Concrete Shell in Slow Granite to an Incident Wave of Rectangular Pressure-profile - - - - -	15
4	Displacement Response of the Concrete Shell in Slow Granite Computed with $\tilde{C}_m = Q$ - - - - -	16
5	Velocity Response of a Concrete Shell in Granite to an Incident Step-wave	18
6	Stress Response in the Middle and Inner Fibers of a Concrete Shell in Granite to an Incident Step-wave - - - - -	19

SECTION I

INTRODUCTION

The treatment of soil-structure interaction is of considerable importance in analyses of the integrity of structures in ground-shock environments. There are currently three basic approaches to the linear treatment of this problem: analytical, lumped-element, and finite-element. Analytical approaches are restricted to very simple geometries; hence, the results are useful for providing insight into the physics of the problem, but the extension to complex geometries is difficult. The lumped-element approach, in which the soil characteristics are represented by discrete masses, springs and dashpots, is economical, but the representation of actual soil behavior is crude. The finite-element (FE) approach can model the problem to almost any accuracy desired, but the large number of elements required precludes efficient computation. An approach to achieve a more versatile and more economical method for the treatment of these problems would combine the best features of the different techniques. Such an approach is pursued in this study: an analytical approximation of the soil-structure interaction is combined with the modeling capabilities of the FE method, while avoiding the burden of many elements in the soil.

This report examines a boundary-element (BE) treatment of the surrounding soil that offers considerable promise for complex soil-structure dynamic analysis. The structure is modeled through the use of an available FE code, and the soil-structure interaction is reduced to a surface relationship through the use of a doubly asymptotic approximation (DAA) [1], which requires the application of BE techniques [2]. The present study focuses on the two-dimensional plane-strain response of structures surrounded by an infinite elastic medium; the extension to more general problems is discussed.

The report first addresses the development of the method: the matrix equation of motion for a structure embedded in an elastic medium is given, the doubly asymptotic surface relationship is presented, and the response equation for the embedded structure is synthesized. Then the solution procedure is discussed, and three numerical examples are considered that illustrate the validity and accuracy of the approach.

SECTION II

GOVERNING EQUATIONS

In this section, governing equations for a finite-element (FE) model of a structure and a boundary-element (BE) formulation of a first-order doubly asymptotic approximation (DAA) for the soil-structure interaction are provided. These equations are then combined to form the response equation for the embedded structure. Finally, computational procedures for the solution of the response equation are discussed.

2.1 STRUCTURAL MODEL

The matrix FE equation of motion for a linear structure embedded in an elastic medium through which an incident disturbance propagates is

$$\underline{\underline{M}}_s \ddot{\underline{q}} + \underline{\underline{K}}_s \underline{q} = -(\underline{f}_I + \underline{f}_S) \quad (1)$$

where $\underline{\underline{M}}_s$ and $\underline{\underline{K}}_s$ are the mass and stiffness matrices for the structure, \underline{q} is the structural displacement vector, \underline{f}_I and \underline{f}_S are surface-force vectors associated with the incident and scattered waves, respectively, and a dot denotes temporal differentiation. The mass and stiffness matrices are easily obtained from any available FE code. The applied load is considered separable into an incident-wave force that would exist if the structure were absent (hence a known quantity), and a scattered-wave force due to the presence of the structure. The scattered-wave force constitutes a troublesome unknown; hence an approximation is introduced for its evaluation.

2.2 DOUBLY ASYMPTOTIC APPROXIMATION

A first-order DAA is introduced to evaluate the scattered-wave force \underline{f}_S [1]. This approximation is a surface interaction approximation, replacing the infinite volume of external medium by a surface coincident with the external surface of the structure. The approximation is asymptotically valid at both high and low frequencies, as are the previously developed approximations for fluid-structure interaction [3,4,5].

The development of a first-order DAA for linear soil-structure interaction proceeds as follows. At high frequencies, each surface element of the discretized structure acts as an infinite flat plate radiating plane waves into the medium. This can be visualized by considering that, for a fixed surface-vibration pattern oscillating at high frequencies, the characteristic propagation wave lengths in the medium are short compared with the characteristic wavelength of the surface-vibration pattern. For normal and tangential motions of the i th surface element, this model yields as scattered-wave surface forces

$$\begin{aligned} g_{Si}^n &= \rho c_d a_i \dot{u}_i^n \\ g_{Si}^t &= \rho c_s a_i \dot{u}_i^t \end{aligned} \quad (2)$$

where ρ is the mass density of the medium, a_i is the surface area of the element, c_d and c_s are the sound speeds for dilatational and shear waves in the medium, respectively, and \dot{u}_i^n and \dot{u}_i^t are the normal and tangential scattered velocities at the surface of the element; see, e.g., [6]. For an assemblage of elements, (2) lead to the matrix relation

$$\underline{g}_S' = \rho \underline{A} \underline{C}_m \underline{\dot{u}}_S' \quad (3)$$

where \underline{A} is a diagonal element-area matrix, \underline{C}_m is a diagonal sound-speed matrix for the medium, and $\underline{\dot{u}}_S'$ is the computational scattered-velocity vector for the surface elements expressed in local coordinates. Upon assembly, the local coordinates in (3) are transformed to the global coordinates for the problem as

$$\underline{\dot{u}}_S' = \underline{G} \underline{\dot{u}}_S \quad (4)$$

From (3), it is clear that the external medium appears to the structure as an added damper in the high-frequency limit.

Low-frequency behavior of the medium is described by the quasi-static surface relation

$$\underline{g}_S = \underline{K}_m \underline{u}_S \quad (5)$$

in which \underline{K}_m is a surface stiffness matrix for the medium. In this limit, the external medium appears to the structure as an added stiffness embodied in \underline{K}_m . The construction of \underline{K}_m is discussed in Section 2.4.

To construct the first-order DAA, (3) and (5) are added to obtain

$$\underline{g}_S = \rho \underline{G}^T \underline{A} \underline{C}_m \underline{G} \underline{\dot{u}}_S + \underline{K}_m \underline{u}_S \quad (6)$$

where the transformation of (3) as $\underline{g}_S = \underline{G}^T \underline{g}_S'$ results from (4) and the fact that virtual work must be independent of the coordinate system used, i.e., $(\delta \underline{u})^T \underline{g} = (\delta \underline{u}')^T \underline{g}'$.

It is easy to see the doubly asymptotic nature of the surface approximation. At low frequencies, the velocity vector is small relative to the displacement vector, so that the scattered force is essentially given by the static stiffness relationship; at high frequencies, the reverse is true, so that the scattered force is essentially given by the radiation damping relationship. In the intermediate frequency range, the DAA is, of course, in error; the purpose of the numerical results presented herein is to indicate the magnitude of that error. If numerical calculations demonstrate the need for an improved approximation, one may be derived; for fluid-structure interaction, an improved DAA has been developed that substantially outperforms the original [5].

2.3 RESPONSE EQUATION

In linear problems, not only is the surface-force vector separable into incident-wave and scattered-wave components [see (1)], but the surface displacement vector \underline{u} is also separable such that $\underline{u} = \underline{u}_I + \underline{u}_S$. Hence (1) and (6) may be combined to give the doubly-asymptotic response equation for the embedded structure

$$\underline{M}_S \ddot{\underline{q}} + \rho \underline{D}^T \underline{G}^T \underline{A} \underline{C}_m \underline{G} \underline{D} \dot{\underline{q}} + (\underline{K}_S + \underline{D}^T \underline{K}_m \underline{D}) \underline{q} = \underline{f}_I + \rho \underline{D}^T \underline{G}^T \underline{A} \underline{C}_m \underline{G} \underline{D} \dot{\underline{u}}_I + \underline{D}^T \underline{K}_m \underline{u}_I \quad (7)$$

where \underline{u} and \underline{f}_S have been transformed as $\underline{u} = \underline{D} \underline{q}$ and $\underline{f}_S = \underline{D}^T \underline{f}_S$, i.e., \underline{D} selects the structural degrees of freedom that define the soil-structure interface. In (7), \underline{M}_S and \underline{K}_S are readily provided by an FE structural analysis code, $\underline{D}^T \underline{G}^T \underline{A} \underline{C}_m \underline{G} \underline{D}$ is easily computed, \underline{f}_I and \underline{u}_I are known, and \underline{K}_m is determined through the application of boundary-integral-equation techniques as now described.

2.4 MEDIUM STIFFNESS MATRIX

The basic boundary-integral equation in two dimensions is [2]

$$\frac{1}{2} \underline{u}^k(P) + \int_L \underline{T}^{k\ell}(P,Q) \underline{u}^\ell(Q) dL(Q) = \int_L \underline{U}^{k\ell}(P,Q) \underline{t}^\ell(Q) dL(Q) \quad (8)$$

where P and Q are surface points, \underline{u}^k and \underline{t}^k are surface displacements and tractions, respectively, $\underline{T}^{k\ell}$ and $\underline{U}^{k\ell}$ are Green's functions for the boundary, and $k = 1, 2$ and $\ell = 1, 2$ are the Cartesian coordinate indices. Through division of the structure's (two-dimensional) external surface into a series of boundary elements, (8) may be expressed in matrix notation as

$$\underline{S} \underline{u} = \underline{F} \underline{t} \quad (9)$$

in which the 2×2 elements of \underline{S} and \underline{F} are given by

$$\begin{aligned} S_{ij}^{k\ell} &= \frac{1}{2} \delta_{ij} \delta_{k\ell} + \int_{L_j} \underline{T}_{ij}^{k\ell} \xi_j^\ell dL_j \\ F_{ij}^{k\ell} &= \int_{L_j} \underline{U}_{ij}^{k\ell} \zeta_j^\ell dL_j \end{aligned} \quad (10)$$

where δ_{ij} and $\delta_{k\ell}$ are Kronecker deltas, i and j are boundary-element indices, ξ_j^ℓ and ζ_j^ℓ are assumed BE shape-functions, and L_j is the length of the j th boundary element. For the two-dimensional plane-strain case, the kernels $\underline{T}_{ij}^{k\ell}$ and $\underline{U}_{ij}^{k\ell}$ are given by [2,7]

$$\begin{aligned} T_{ij}^{k\ell} &= \frac{C_3}{r_{ij}} \left[\frac{\partial r_{ij}}{\partial n_j} (\delta_{k\ell} C_4 + 2 r_{ij,k} r_{ij,\ell}) + C_4 (n_j^k r_{ij,\ell} - n_j^\ell r_{ij,k}) \right] \\ U_{ij}^{k\ell} &= C_1 (\delta_{k\ell} C_2 \ln r_{ij} - r_{ij,k} r_{ij,\ell}) \end{aligned} \quad (11)$$

where C_1, C_2, C_3 and C_4 are material constants, r_{ij} is the distance from a node point on the i th element to the variable (field) point of integration on the j th element, n_j is the unit normal to the surface of the j th element, n_j^k is the cosine of the angle between n_j and the k th Cartesian direction, and a subscript following a comma represents spatial differentiation with respect to the indicated Cartesian coordinate at point j . In the present implementation, the displacement and traction shape-functions ξ_j^k and ζ_j^k are assumed to be constant over the j th element, so they may be brought out from under the integral signs in (10). The numerical techniques used to evaluate the integrals in (10) are discussed in the appendix.

Once the matrices in (9) have been generated, it is a simple matter to obtain the medium stiffness matrix; because \underline{F} is nonsingular, it can be factored to obtain

$$\underline{t} = \underline{F}^{-1} \underline{S} \underline{u} = \underline{K}_m \underline{u} \quad (12)$$

As the preceding development is not based on variational principles, the derived stiffness matrix may not be symmetric; therefore \underline{K}_m is symmetrized before it is used in (7).

The brevity of the preceding BE formulation is appropriate, in view of the extensive coverage of the subject provided in [2]. The emphasis here has been on the specific approach of this study; it has been found to be most economical, especially the use of numerical integration to evaluate the matrix elements defined in (10). The apparently new technique of using boundary integral equations to define a medium stiffness matrix is valuable, in that it facilitates the use of the form (12). This form is required for an efficient marriage of an FE structural model and a BE soil model. There are also improved forms of the BE method available that utilize higher order shape-functions to describe boundary displacements and tractions, as well as sophisticated isoparametric-element representations; these procedures are reviewed by Cruse [8]. The simple approach used in this study is, however, adequate for the purposes of the present investigation. If software were to be constructed for production analysis, the incorporation of refined BE techniques would be appropriate.

2.5 SOLUTION PROCEDURE

The doubly asymptotic response equation for the embedded structure, (7), has the form of the standard matrix equation of structural dynamics; hence, the solution of (7) may be accomplished with well-established techniques. For the linear response problems considered here, the integration of (7) is performed in accordance with the trapezoidal rule [9]. The equation solver used with the time integrator is the skyline format procedure of Felippa [10].

A study of (7) on a term-by-term basis is informative. The mass matrix produced by REXBAT [11], the structural finite-element code used in this study, is diagonal; a consistent mass matrix could be used, however, without unduly complicating the solution. The damping matrix is highly banded in all cases and presents no computational difficulties. The stiffness matrix, on the other hand, may be nearly full, due to the added stiffness terms. (Note that the matrices generated from (10) are full.) For the simple examples considered here, this dense stiffness matrix presents no difficulty. However, for large systems, the compact bandwidth (low connectivity) of the structural model, which is needed for efficient solution, would be lost through the addition of the fully populated medium stiffness matrix. To overcome this problem, a staggered-solution approach, such as the one developed for fluid-structure interaction analysis by Park, et al. [12] should be considered for large systems of equations. The forcing function, i.e., the right side of (7), may look complicated, but each term is known and the load vector is easily computed by simple matrix-vector multiplication and vector addition.

The power of the present approach is certainly evident for engineering applications, as the FE and BE methods enjoy direct applicability to the complex geometries of engineering structures. Furthermore, the doubly asymptotic response equation for the embedded structure is merely the second-order ordinary differential equation of structural dynamics.

SECTION III

NUMERICAL RESULTS

In this section, numerical results for the transverse excitation of an infinite, circular cylindrical cavity and for two infinite, circular cylindrical shells by an incident plane, dilatational wave are compared with corresponding analytical solutions. Problem geometry and notation are shown in Figure 1; in all cases, plane strain response is assumed. The coincident finite-element and boundary-element grids for all three problems consist of 40 elements of equal length. The finite-element shell models incorporate straight beam elements with elastic moduli modified for replication of plane strain conditions.

The results are presented in nondimensional form. Length is normalized to a , time is normalized to a/c_d , and stress is normalized to $\rho c_d^2 = \lambda + 2\mu$, where λ and μ are the Lamé coefficients for the medium.

3.1 INCIDENT WAVE

A plane dilatational step-wave, characterized by a compressive pressure P_0 and moving in the x_1 -direction, can be described in terms of a nondimensional scalar potential ϕ_I as

$$\phi_I = -\frac{1}{2} P_0 (\tau - x_1 - 1)^2 H(\tau - x_1 - 1) \quad (13)$$

where τ is nondimensional time, x_1 is nondimensional position along the x_1 axis, and H is the Heavyside operator. For this incident wave, the shear potential is zero [6].

The incident-wave force vector \underline{f}_I , which appears on the right side of (7), is obtained as follows. First, the elements of the incident-wave computational stress vector in global (x_1, x_2) coordinates are determined by application of classical continuum formulas to (13) [6]; this yields

$$\begin{aligned} \sigma_{Ii}^k &= -(\lambda + 2\mu \delta_{1k}) P_0 H(\tau - x_{1i} - 1) \\ \tau_{Ii}^{k\ell} &= 0 \end{aligned} \quad (14)$$

where x_{1i} denotes the x_1 -position of the i th surface node. Second, a global stress vector is constructed from these elements, which is then transformed, on the basis of Mohr's circle, into local coordinates as $\underline{\sigma}'_I = \underline{M} \underline{\sigma}_I$. Finally, the force vector in local coordinates is determined as $\underline{f}'_I = -\underline{A} \underline{\sigma}'_I$, which is then transformed into global coordinates to yield [c.f., (6)]

$$\underline{f}_I = -\underline{G}^T \underline{A} \underline{M} \underline{\sigma}_I \quad (15)$$

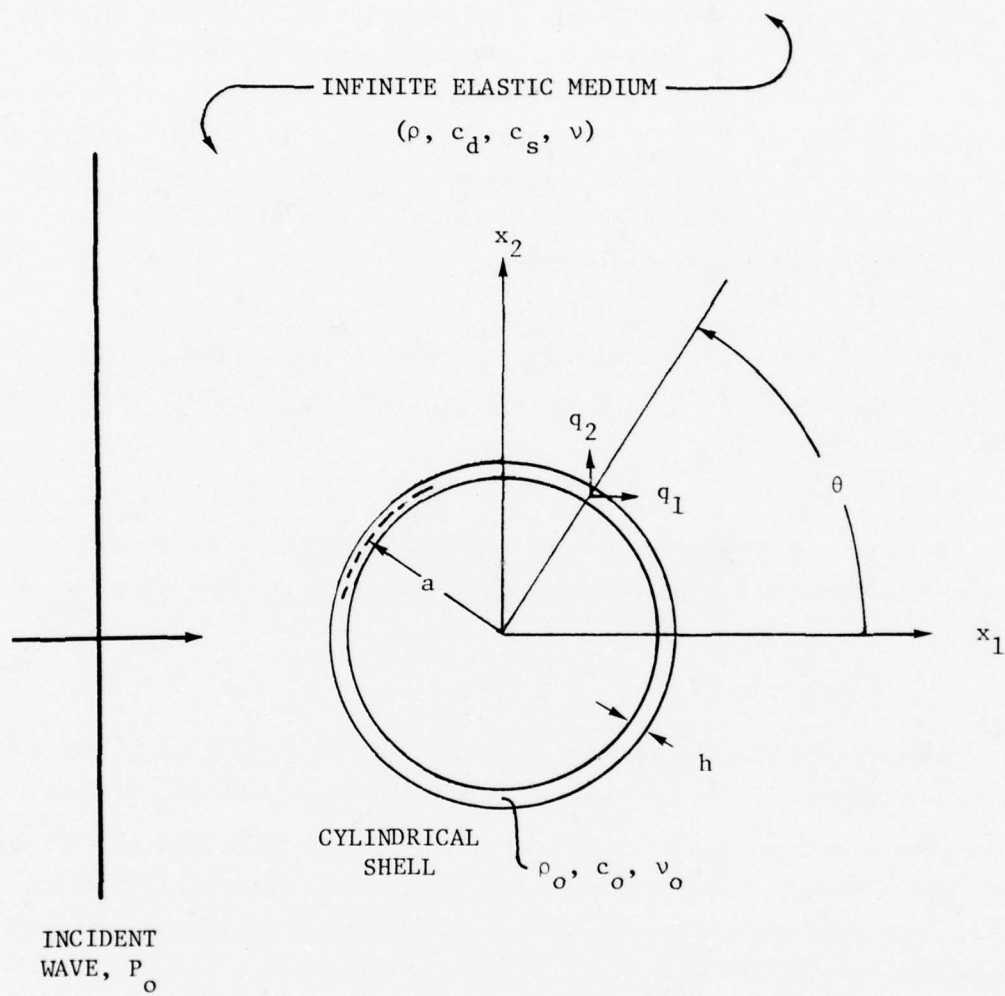


Figure 1. Geometry and Notation for the Check Problems.

The incident-wave displacement and velocity vectors \underline{u}_I and $\dot{\underline{u}}_I$, which also appear on the right side of (7), are obtained from the classical relation $u^k = \partial \phi / \partial x_k$. This relation and (13) yield as the elements of these vectors

$$\begin{aligned} u_{Ii}^k &= \delta_{lk} P_o (\tau - x_{li} - 1) H(\tau - x_{li} - 1) \\ \dot{u}_{Ii}^k &= \delta_{lk} P_o H(T - x_{li} - 1) \end{aligned} \quad (16)$$

3.2 CIRCULAR CAVITY

The cavity problem is formulated simply by taking $\underline{M}_s = \underline{K}_s = 0$, which reduces (7) to a first-order equation. A comparison between results obtained by the present method and analytical results presented in [13] is provided, for step-wave excitation, in Figure 2. Minor discrepancies exist between the DA/BE and analytical response histories at early times. At late times, both sets of response histories approach the appropriate asymptotes [1, 14]; these asymptotes are $\tau-4$, $\tau-1$ and $\tau+2$ for $\theta=0^\circ$, 90° , and 180° , respectively.

3.3 CONCRETE SHELL IN SLOW GRANITE

The second check problem, the response of a concrete shell to an incident wave of rectangular pressure-profile, is also taken from [13]. The nondimensional parameters for this problem are $h/a = 0.01$, $\rho_o/\rho = 0.865$, $c_s/c_d = 0.63$, $c_o/c_d = 1.87$, $\nu = 0.25$, and $\nu_o = 0.2$; the duration of the incident rectangular pulse is 10. DA/BE and analytical displacement histories for this problem are compared in Figure 3. In this figure, as in Figure 2, the DA/BE responses generally tend to lag behind their analytical counterparts. As discussed in [1], this tendency is the result of excess radiation damping introduced by the DAA. Also of interest is the DA/BE prediction of shell response at $\theta=0^\circ$ before $\tau=1.53$, which is the earliest time a disturbance can reach that point [15]; this nonphysical result illustrates that the DAA is not a wave propagation approximation. Despite its deficiencies, however, the DAA produces results that nowhere differ from their analytical counterparts by more than 10% of the peak response and also approach the proper late-time asymptote. The latter characteristic attests to the correctness of the \underline{K}_m -calculation.

Although the DAA tends to overestimate radiation damping, its inclusion is absolutely necessary for an accurate treatment of abrupt soil-structure interaction. This is indicated in Figure 4, where displacement responses corresponding to the DA/FE responses of Figure 3 have been computed from (7) with \underline{C}_m set equal to $\underline{0}$. As one would expect, the highly oscillatory response thus calculated produces extremely poor stress/strain results.

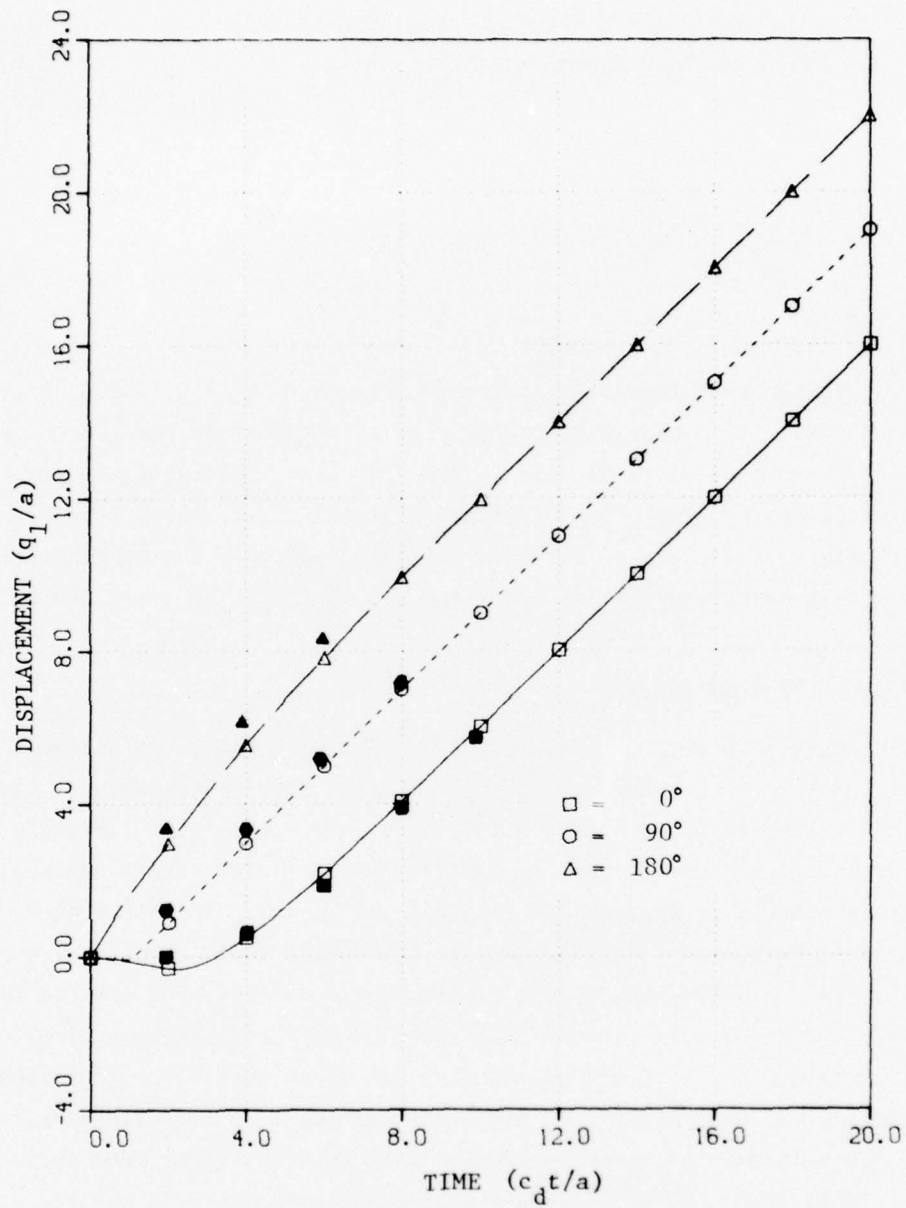


Figure 2. Displacement Response of a Circular Cavity to an Incident Step-wave [solid symbols denote results from (13)].

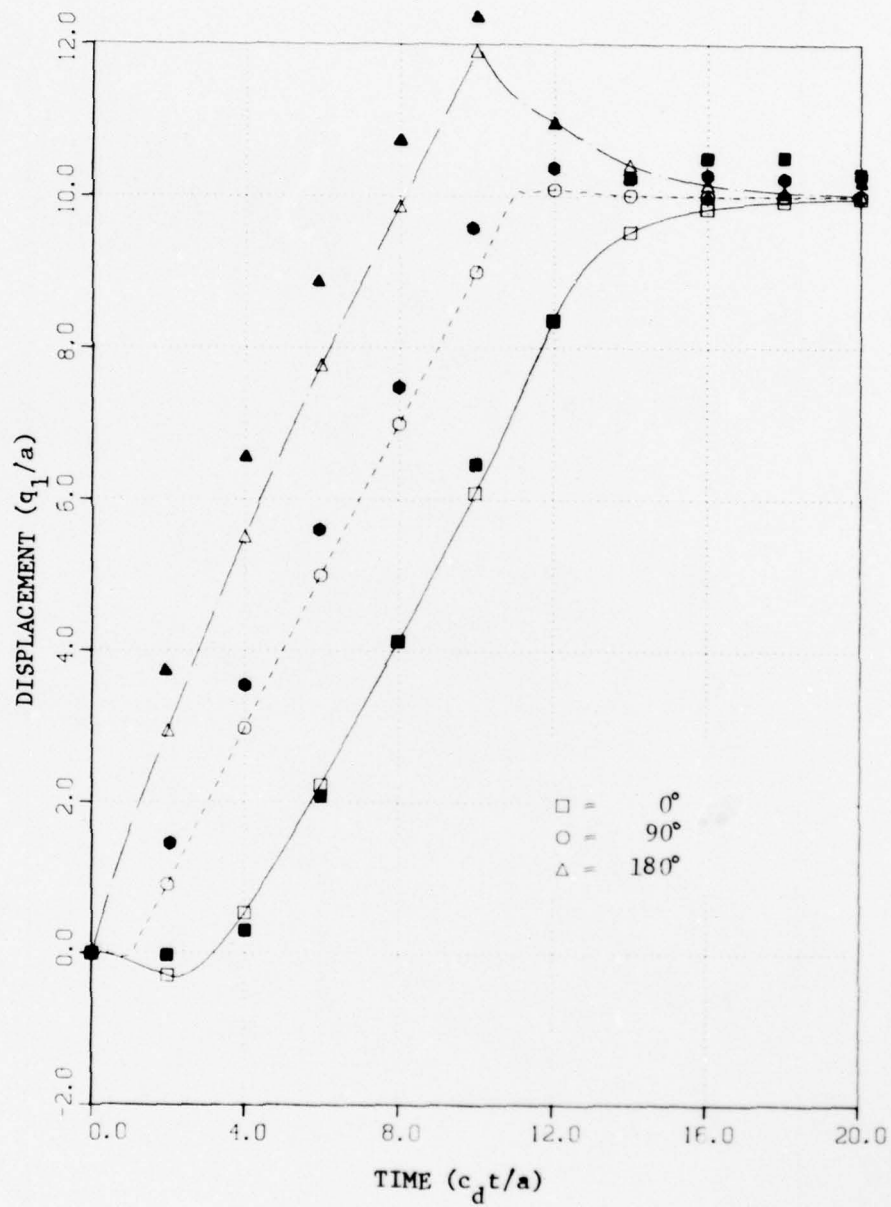


Figure 3. Displacement Response of a Concrete Shell in Slow Granite to an Incident Wave of Rectangular Pressure-profile [solid symbols denote results from (13)].

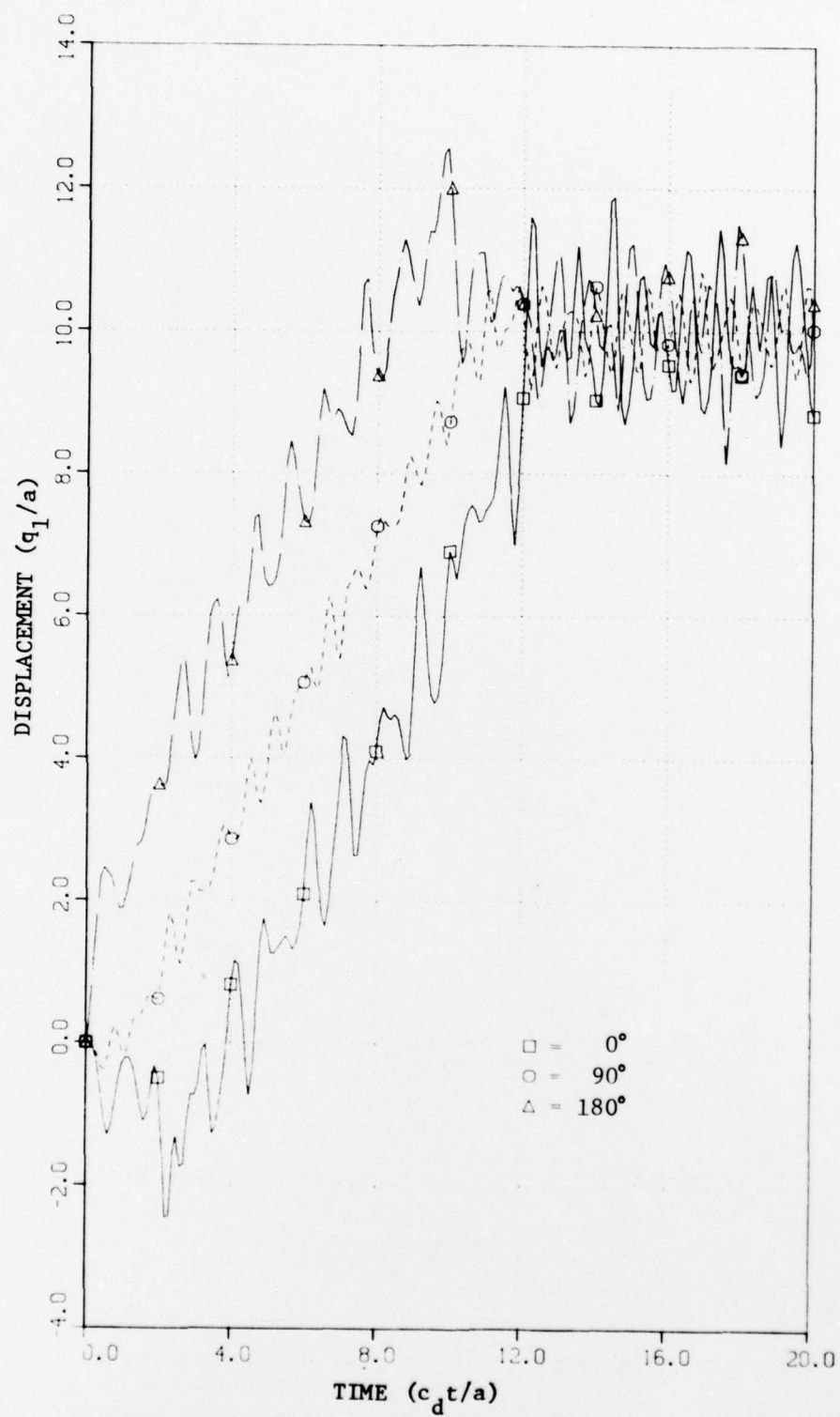


Figure 4. Displacement Response of the Concrete Shell in Slow Granite Computed with $\zeta_m = 0$.

3.4 CONCRETE SHELL IN GRANITE

The final check problem, the response of a concrete shell to an incident step-wave, is taken from [1]. The appropriate nondimensional parameters here are $h/a = 0.05$, $\rho_o/\rho = 1.0$, $c_s/c_d = 1/\sqrt{3}$, $c_o/c_d = 1/\sqrt{2}$, and $v = v_o = 0.25$. Velocity response histories at $\theta = 0^\circ$ & 180° are shown in Figure 5, corresponding to DA/BE, DA/analytical and exact/analytical treatments of the structure-medium interaction. It is seen that the DA/BE and DA/analytical results are in almost perfect agreement, which is most reassuring. Premature initial response at points in the shadow region and excessive radiation damping characterize the DA results here as they did in Figure 3. The associated error is modest, however, with all results coalescing at late times. Stress response histories in the middle and inner fibers of the shell at $\theta = 90^\circ$ are shown in Figure 6. Here, some minor discrepancies between the DA/BE and DA/analytical results appear: near $\tau = 0$, the DA/BE histories exhibit a more realistic delay before a stress response appears; near $\tau = 1.5$, short-term reversals in stress appear in the DA/BE histories, whereas the analytical histories are smooth; finally, at late times, the DA/BE asymptotic stress values are slightly less than their analytical counterparts. Much larger discrepancies exist between the DA results and the exact results, especially during the period $4 \leq \tau \leq 12$. Even here, however, the error never exceeds 15%, which is generally acceptable for engineering analysis.

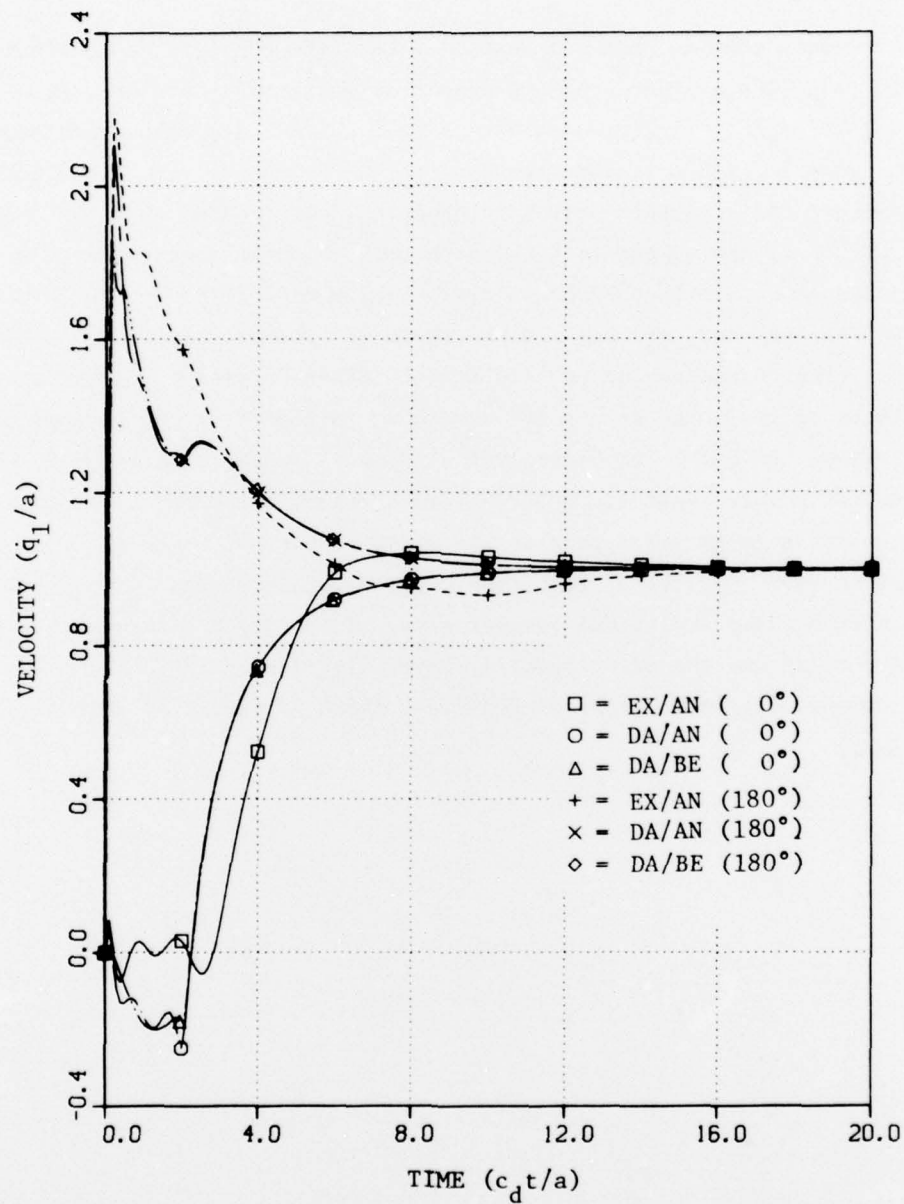


Figure 5. Velocity Response of a Concrete Shell in Granite to an Incident Step-wave (Exact/Analytical, DA/Analytical, DA/BE).

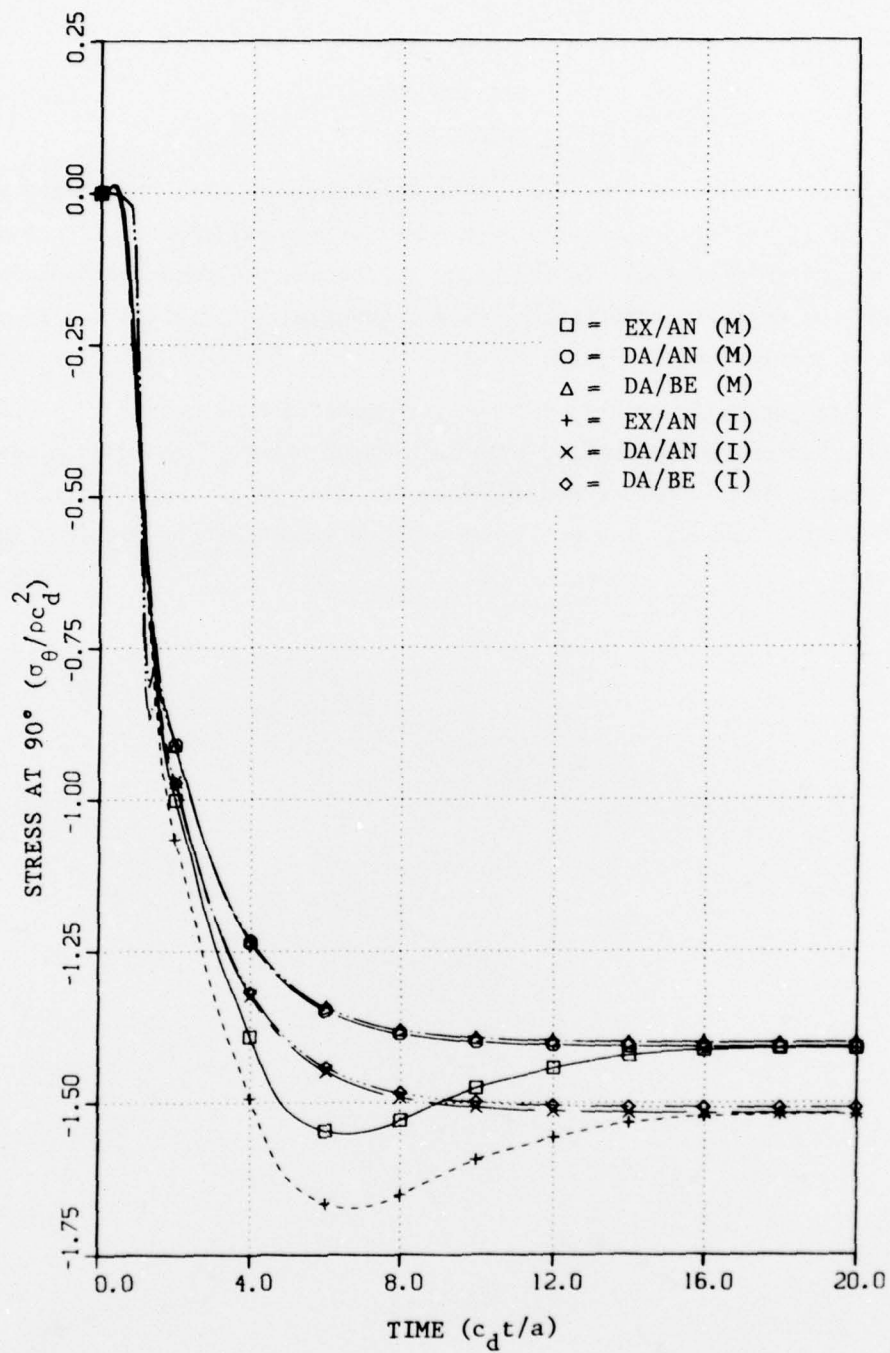


Figure 6. Stress Response in the Middle and Inner Fibers of a Concrete Shell in Granite to an Incident Step-Wave (Exact/Analytical, DA/Analytical, and DA/BE).

SECTION IV

CONCLUSION

The numerical results of the previous section indicate that the doubly asymptotic approximation of [1] offers considerable promise for the satisfactory treatment of dynamic soil-structure interaction. In addition, the boundary-element methods described in Section II and the Appendix constitute a firm technology for application to engineering structures with complex surface geometries.

The extension of DA/BE methods for the treatment of nonlinear soil response is discussed in [16]. As one would expect, this is a major effort, requiring consideration of the state of the medium at points removed from the surface of the structure. In spite of the difficulties, however, the nonlinear problem appears to be yielding to the new methods.

REFERENCES

1. T. L. Geers and C.-L. Yen, "Transient Excitation of an Elastic Cylindrical Shell Embedded in an Elastic Medium: Residual Potential and Doubly Asymptotic Solutions", DNA report in preparation.
2. T. A. Cruse and F. J. Rizzo, eds., Boundary Integral Equation Method: Computational Applications in Applied Mechanics, AMD-Vol. 11, ASME, New York, 1975.
3. T. L. Geers, "Residual Potential and Approximate Methods for Three-Dimensional Fluid-Structure Interaction Problems", J. Acoust. Soc. Am., 49, 1505-1510, 1971.
4. T. L. Geers, "Transient Response Analysis of Submerged Structures", pp. 59-84 of Finite Element Analysis of Transient Nonlinear Structural Behavior, AMD-Vol. 14, ASME, New York, 1975.
5. T. L. Geers, "Doubly Asymptotic Approximations for Transient Motions of Submerged Structures", to appear in J. Acoust. Soc. Am.
6. J. D. Achenbach, Wave Propagation in Elastic Solids, North-Holland Publishing Company, Amsterdam, 1973.
7. F. J. Rizzo, "An Integral Equation Approach to Boundary Value Problems of Classical Elastostatics", Quart. Appl. Math., 25, 83-95, 1967.
8. T. A. Cruse and R. B. Wilson, "Advanced Applications of Boundary Integral Equation Methods", Proc. 4th. Int. Conf. on Structural Mechanics in Reactor Technology, San Francisco, 15-19 August 1977.
9. C. A. Felippa and K. C. Park, "Computational Aspects of Time Integration Procedures in Structural Dynamics", to appear in J. Appl. Mech.
10. C. A. Felippa, "Solution of Linear Equations with Skyline-Stored Symmetric Matrix", Computers & Structures, 5, 13-29, 1975.
11. W. A. Loden and L. E. Stearns, "User's Manual for the REXBAT Program", LMSC-D460625, Lockheed Missiles and Space Co., Sunnyvale, Ca., January 1976.
12. K. C. Park, C. A. Felippa, and J. A. DeRuntz, "Stabilization of Staggered Solution Procedures for Fluid-Structure Interaction Analysis", pp. 95-124 of Computational Methods for Fluid Structure Interaction Problems, AMD-Vol. 26, ASME, New York, 1977;
13. H. Garnet and J. Crouzet-Pascal, "Transient Response of a Circular Cylinder of Arbitrary Thickness, in an Elastic Medium, to a Plane Dilatational Wave", J. Appl. Mech., 33, 521-531, 1966.
14. T. Yoshihara, A. R. Robinson, and J. L. Merritt, "Interaction of Plane Elastic Waves with an Elastic Cylindrical Shell", Structure Research Series Rpt. No. 261, University of Illinois, Urbana, January 1963.
15. T. L. Geers, "Scattering of a Transient Acoustic Wave by an Elastic Cylindrical Shell", J. Acoust. Soc. Am., 51, 1640-1651, 1972.
16. P. G. Underwood, "Two-Dimensional, Doubly Asymptotic Analysis of Dynamic, Nonlinear, Soil-Structure Interaction", DNA report in preparation.
17. G. Dahlquist and A. Bjork, Numerical Methods, Prentice-Hall, Inc., Englewood Cliffs, N.J., 1974.

APPENDIX

This appendix discusses the numerical approach used to evaluate the integrals in (10) for determination of the matrix elements S_{ij}^{kl} and F_{ij}^{kl} .

First, the boundary is divided into 2-D boundary elements, each with a centrally located node. For a single calculation of S_{ij}^{kl} and F_{ij}^{kl} , fixed values are assigned to i, j, k and ℓ , and a circle is fitted to the nodal points $j-1, j$ and $j+1$; this completely determines the center and radius of the arc describing the j th element. The ends of the j th element are then point $j-\frac{1}{2}$ on the arc half-way between points $j-1$ and j and point $j+\frac{1}{2}$ on the arc half-way between points j and $j+1$. Hence L_j is the arc length between points $j-\frac{1}{2}$ and $j+\frac{1}{2}$, and the unit normal anywhere on the element is completely defined.

Second, the displacement and traction shape-functions, ξ_j^ℓ and ζ_j^ℓ , are taken as unity, so the integrals in (10) only involve the kernels (11). In this connection, it is important to remember that T_{ij}^{kl} and U_{ij}^{kl} pertain to a fixed point (the nodal point) on the i th element, but to a variable point on the j th element. For $j \neq i$, the geometric quantities in (11) are easily determined as

$$\begin{aligned} r_{ij} &= \left[(x_{1i} - x_{1j})^2 + (x_{2i} - x_{2j})^2 \right]^{\frac{1}{2}} \\ r_{ij,k} &= (x_{kj} - x_{ki}) / r_{ij} \\ \frac{\partial r_{ij}}{\partial n_j} &= n_j^1 r_{ij,1} + n_j^2 r_{ij,2} \end{aligned} \quad (17)$$

and Simpson's rule is used to evaluate the integrals with points $j-\frac{1}{2}, j$ and $j+\frac{1}{2}$ as the integration points. For $j = i$, special evaluation methods are used, as described in the following paragraph.

With regard to the integral of T_{ii}^{kl} , it may be shown [7] that [see (11)]

$$\begin{aligned} \int_{L_i}^{-1} r_{ii}^{-1} \frac{\partial r_{ii}}{\partial n_i} (\delta_{kl} C_4 + 2r_{ii,k} r_{ii,\ell}) dL_i &= -\pi(C_4 + 1) \delta_{kl} \\ \int_{L_i} (n_i^k r_{ii,\ell} - n_i^\ell r_{ii,k}) dL_i &= 0 \end{aligned} \quad (18)$$

where the first i -subscript of the doubly subscripted variable r_{ii} refers to the fixed nodal point for the i th element, and the second i -subscript of r_{ii} and any single i -subscript refers to a variable point on that element. With regard to the integral of

$U_{ii}^{k\ell}$, it may be shown that [see (11)]

$$\int_{L_i} \ln r_{ii} dL_i = r_{i(i-\frac{1}{2})} \left(\ln r_{i(i-\frac{1}{2})} - 1 \right) + r_{i(i+\frac{1}{2})} \left(\ln r_{i(i+\frac{1}{2})} - 1 \right) \quad (19)$$

where the subscripts $(i-\frac{1}{2})$ and $(i+\frac{1}{2})$ refer to the end points of the i th element. Integration of the second term in the expression for $U_{ii}^{k\ell}$ [see (11)] is performed by means of Simpson's rule, with the nodal point i and the end points $i-\frac{1}{2}$ and $i+\frac{1}{2}$ as integration points. In this exercise, the second of (17) is used directly to evaluate $r_{ii,k}$ $r_{ii,\ell}$ at the end points, while it is used at the nodal point in conjunction with a Richardson extrapolation [17] of the form

$$\begin{aligned} r_{ii,k}^{(n)} r_{ii,\ell}^{(n)} = \frac{1}{2} & \left[-r_{i(i-\epsilon),k} r_{i(i-\epsilon),\ell} + 2r_{i(i-2\epsilon),k} r_{i(i-2\epsilon),\ell} \right. \\ & \left. + 2r_{i(i+2\epsilon),k} r_{i(i+2\epsilon),\ell} - r_{i(i+\epsilon),k} r_{i(i+\epsilon),\ell} \right] \end{aligned} \quad (20)$$

where $r_{i(i-\epsilon),k}$, for example, denotes the value of $r_{ii,k}$ [obtained from the second of (17)] that pertains to the i th nodal point and to a fixed point located between the nodal points $i-1$ and i at a distance ϵ from nodal point i ; here, ϵ has been taken as $0.05 L_i$.

Finally, each value of $F_{ij}^{k\ell}$ is scaled through division by L_j . This scales the tractions t_j^k so that they, in effect, become nodal forces, producing a stiffness matrix K_m of the standard FE form.

DISTRIBUTION LIST

DEPARTMENT OF DEFENSE

Assistant to the Secretary of Defense
Atomic Energy
ATTN: Col R. Brodie
ATTN: ATSD (AE)

Director
Defense Advanced Rsch. Proj. Agency
ATTN: STO
ATTN: NMRO
ATTN: PMO
ATTN: Technical Library

Director
Defense Civil Preparedness Agency
ATTN: G. Sisson
ATTN: Admin. Officer

Director
Defense Communications Agency
ATTN: Code 930
ATTN: CCTC/C672

Defense Documentation Center
Cameron Station
12 cy ATTN: TC

Director
Defense Intelligence Agency
ATTN: DB-4C1
ATTN: DC-1C
ATTN: DB-4C2, T. Ross
ATTN: DB-4C3
ATTN: Technical Library
ATTN: DT-2, Wpns. & Sys. Div.

Director
Defense Nuclear Agency
ATTN: DDST
ATTN: TISI
2 cy ATTN: SPSS
2 cy ATTN: SPAS
3 cy ATTN: TITL

Commander
Field Command, Defense Nuclear Agency
ATTN: FCPR
ATTN: FCTMOF

Director
Interservice Nuclear Weapons School
ATTN: Document Control

Director
Joint Strat. Tgt. Planning Staff
ATTN: DOXT
ATTN: STINFO Library
ATTN: JLTW-2
ATTN: XPFS

Chief
Livermore Division, Fld. Command, DNA
ATTN: FCPRL

DEPARTMENT OF DEFENSE (Continued)

Chief
Test Construction Division
Field Command Test Directorate
ATTN: FCTC

Under Sec'y of Def. for Rsch. & Engrg.
ATTN: S&SS (OS)

DEPARTMENT OF THE ARMY

Director
BMD Advanced Tech. Ctr.
ATTN: 1CRDABH-X
ATTN: CRDABH-S

Program Manager
BMD Program Office
ATTN: CRDABM-NF

Commander
BMD System Command
ATTN: BDMSC-TEN, N. Hurst

Director
Construction Engineering Rsch. Lab.
ATTN: CERL-SL

Dep. Chief of Staff for Rsch. Dev. & Acq.
ATTN: Technical Library
ATTN: DAMA(CS), Maj A. Gleim
ATTN: DAMA-CSM-N, LTC G. Ogden

Chief of Engineers
ATTN: DAEN-RDM
ATTN: DAEN-MCE-D

Deputy Chief of Staff for Ops. & Plans
ATTN: Dir. of Chem. & Nuc. Ops.
ATTN: Technical Library

Chief
Engineer Strategic Studies Group
ATTN: DAEN-FES, LTC Hatch

Commander
ERADCOM Technical Support Directorate
ATTN: DRSEL-TL-IR, E. Hunter

Commander
Harry Diamond Laboratories
ATTN: DELHD-TI, Technical Library
ATTN: DELHD-NP

Commander
Redstone Scientific Information Ctr.
ATTN: Chief, Documents

Commander
US Army Armament Command
ATTN: Technical Library

DEPARTMENT OF THE ARMY (Continued)

Director

US Army Ballistic Research Labs.

ATTN: A. Ricchiazzi

ATTN: DRDAR-BLE, J. Keefer

ATTN: C. Kingery

ATTN: DRDAR-BLE, W. Taylor

ATTN: DRXBR-X, J. Meszaros

2 cy ATTN: Technical Library, E. Baicy

Commander

US Army Comb. Arms Combat Dev. Acty.

ATTN: LTC G. Steger

ATTN: LTC Pullen

Commander

US Army Communications Cmd.

ATTN: Technical Library

Commander

US Army Engineer Center

ATTN: ATSEN-SY-L

Division Engineer

US Army Engineer Div., Huntsville

ATTN: HNDED-SR

Division Engineer

US Army Engineer Div., Ohio River

ATTN: Technical Library

Commandant

US Army Engineer School

ATTN: ATSE-TEA-AD

ATTN: ATSE-CTD-CS

Director

US Army Engr. Waterways Exper. Sta.

ATTN: J. Ballard

ATTN: G. Jackson

ATTN: W. Flathau

ATTN: J. Strange

ATTN: L. Ingram

ATTN: Technical Library

ATTN: F. Brown

Commander

US Army Foreign Science & Tech. Ctr.

ATTN: Research & Concepts Branch

Commander

US Army Mat. & Mechanics Rsch. Ctr.

ATTN: Technical Library

ATTN: J. Mescall

ATTN: R. Shea

Commander

US Army Materiel Dev. & Readiness Cmd.

ATTN: DRCDF-D, L. Flynn

ATTN: Technical Library

Commander

US Army Missile R&D Command

ATTN: DRDMT-XS, Chief Scientist

ATTN: J. Hogan

Commander

US Army Mobility Equip. R&D Ctr.

ATTN: Technical Library

ATTN: A. Tolbert

DEPARTMENT OF THE ARMY (Continued)

Commander

US Army Nuclear & Chemical Agency

ATTN: Library

Commander

US Army Training and Doctrine Cmd.

ATTN: LTC J. Foss

ATTN: LTC Auveduti, COL Enger

Commandant

US Army War College

ATTN: Library

US Army Mat. Cmd. Proj. Mngr. for Nuc. Munitions

ATTN: DRCPM-NUC

DEPARTMENT OF THE NAVY

Chief of Naval Material

ATTN: MAT 0323

Chief of Naval Operations

ATTN: OP 982, CAPT Toole

ATTN: Code 604C3, R. Piacesi

ATTN: OP 03EG

ATTN: OP 981

ATTN: OP 982, Lt Col Dubac

ATTN: OP 098T8

ATTN: OP 982, LCDR Smith

Chief of Naval Research

ATTN: Code 464, T. Quinn

ATTN: Code 463, J. Heacock

ATTN: Code 461, J. Warner

ATTN: Technical Library

ATTN: Code 474, N. Perrone

Officer-in-Charge

Civil Engineering Laboratory

Naval Construction Battalion Center

ATTN: W. Shaw

ATTN: Technical Library

ATTN: R. Odello

ATTN: S. Takahashi

Commandant of the Marine Corps

ATTN: POM

Commander

David W. Taylor Naval Ship R&D Ctr.

ATTN: Code 2740, Y. Wang

ATTN: Code 1700, W. Murray

ATTN: R. Short

ATTN: Code L42-3, Library

ATTN: Code 177, E. Palmer

ATTN: Code 1740-5, B. Whang

Commanding General

Development Center

ATTN: CAPT Hartneady

ATTN: Lt Col Gapenski

Commander

Naval Air Systems Command

ATTN: F. Marquardt

Commander

Naval Electronic Systems Command

ATTN: PME 117-21A

DEPARTMENT OF THE NAVY (Continued)

Commanding Officer
Naval Explosive Ord. Disposal Fac.
ATTN: Code 504, J. Petrousky

Commander
Naval Facilities Engineering Command
ATTN: Code 04B
ATTN: Technical Library
ATTN: Code 03A

Commander
Naval Ocean Systems Center
ATTN: Technical Library
ATTN: E. Cooper

Superintendent (Code 1424)
Naval Postgraduate School
ATTN: Code 2124, Tech. Rpts. Librarian

Director
Naval Research Laboratory
ATTN: Code 2600, Technical Library
ATTN: Code 8440, F. Rosenthal

Commander
Naval Sea Systems Command
ATTN: ORD-033
ATTN: SEA-9931G
ATTN: Code 03511
ATTN: ORD-91313 Library

Commander
Naval Ship Engineering Center
ATTN: NSEC 6105G
ATTN: Technical Library

Officer-in-Charge
Naval Surface Weapons Center
ATTN: Code WA501, Navy Nuc. Prgms. Off.
ATTN: Code 240, C. Aronson
ATTN: G. Matteson
ATTN: M. Kleinerman

Commander
Naval Surface Weapons Center
Dahlgren Laboratory
ATTN: Technical Library

Naval War College
ATTN: Technical Library

Commander
Naval Weapons Center
ATTN: Code 533, Technical Library

Commanding Officer
Naval Weapons Evaluation Facility
ATTN: Technical Library
ATTN: R. Hughes

Director
Strategic Systems Project Office
ATTN: NSP-43, Technical Library
ATTN: NSP-273
ATTN: NSP-272

DEPARTMENT OF THE AIR FORCE

Commander, ADCOM/DC
ATTN: KRX

DEPARTMENT OF THE AIR FORCE (Continued)

AF Geophysics Laboratory, AFSC
ATTN: SUOL, Rsch. Library
ATTN: LWW, K. Thompson

AF Institute of Technology, AU
ATTN: Library, AFIT, Bldg. 640, Area B

AF Weapons Laboratory, AFSC
ATTN: Dep, J. Bratton
ATTN: DES-G, Mr. Melzer
ATTN: DES-S, M. Plamondon
ATTN: DES-C, R. Henny
ATTN: Lt Col J. Leech
ATTN: DED

Headquarters
Air Force Systems Command
ATTN: R. Cross
ATTN: DLCAW

Commander
ASD
ATTN: Technical Library

Assistant Secretary of the Air Force
Research and Development
ATTN: Col R. Steere

Deputy Chief of Staff
Research and Development
ATTN: Col J. Gilbert

Commander
Foreign Technology Division, AFSC
ATTN: PDBG
ATTN: NICD, Library
ATTN: FTDP
ATTN: PDBF, Mr. Spring

HQ USAF/IN
ATTN: IN

HQ USAF/PR
ATTN: PRE

HQ USAF/RD
ATTN: RDPS, Lt Col A. Chiota
ATTN: RDQRM, Col S. Green
ATTN: RDPM
ATTN: RDQPN, Maj F. Vajda
ATTN: RDQSM

Commander
Rome Air Development Center, AFSC
ATTN: FMTLD, Document Library
ATTN: RBES, R. Mair

SAMSO/DE
ATTN: DEB

SAMSO/DY
ATTN: DYS

SAMSO/MN
ATTN: MNH
ATTN: MMH

SAMSO/RS
ATTN: RSS/Col D. Dowler

DEPARTMENT OF THE AIR FORCE (Continued)

Commander in Chief
Strategic Air Command
ATTN: NRI-STINFO, Library

DEPARTMENT OF ENERGY

Albuquerque Operations Office
ATTN: Doc. Con. for Technical Library

Division of Headquarters Services
ATTN: Doc. Con. for Class Technical Library

Nevada Operations Office
ATTN: Doc. Con. for Technical Library

Division of Military Application
ATTN: Doc. Con. for Test Office

University of California
Lawrence Livermore Laboratory
ATTN: Doc. Con. for T. Butkovich
ATTN: Doc. Con. for J. Goudreau
ATTN: Doc. Con. for M. Fernandez
ATTN: Doc. Con. for T. Gold
ATTN: Doc. Con. for J. Thomsen
ATTN: Doc. Con. for L-96, L. Woodruff
ATTN: Doc. Con. for L-205, J. Hearst
ATTN: Doc. Con. for L-200, J. Cortez
ATTN: Doc. Con. for L-90, D. Norris
ATTN: Doc. Con. for L-437, R. Schock
ATTN: L-3, Technical Info. Dept.
ATTN: Doc. Con. for L-7, J. Kahn
ATTN: Doc. Con. for L-90, R. Dong

Los Alamos Scientific Laboratory
ATTN: Doc. Con. for A Davis
ATTN: Doc. Con. for T. Dowler
ATTN: Doc. Con. for G. Spillman
ATTN: Doc. Con. for Reports Library

Oak Ridge National Laboratory
Union Carbide Corporation - Nuclear Division
ATTN: Doc. Con. for Technical Library
ATTN: Doc. Con. for Civil Def. Res. Proj.

Sandia Laboratories, Livermore Laboratory
ATTN: Doc. Con. for Technical Library

Sandia Laboratories
ATTN: Doc. Con. for W. Caudle
ATTN: Doc. Con. for L. Vortman
ATTN: Doc. Con. for W. Roherty
ATTN: Doc. Con. for L. Hill
ATTN: Doc. Con. for W. Herrmann
ATTN: Doc. Con. for 3141, Sandia Rpt. Coll.
ATTN: Doc. Con. for A. Chaban

OTHER GOVERNMENT AGENCIES

Central Intelligence Agency
ATTN: RD/SI, Rm. 5G48, HQ. Bldg. for
NED/OSI-5G48, HQS

Department of the Interior, Bureau of Mines
ATTN: Technical Library

NASA, Ames Research Center
ATTN: R. Jackson

OTHER GOVERNMENT AGENCIES (Continued)

Office of Nuclear Reactor Regulation
Nuclear Regulatory Commission
ATTN: L. Shao
ATTN: R. Heineman

DEPARTMENT OF DEFENSE CONTRACTORS

Aerospace Corp.
ATTN: L. Selzer
ATTN: P. Mathur
2 cy ATTN: Tech. Info. Services

Agabian Associates
ATTN: C. Bagge
ATTN: M. Agabian

Analytic Services, Inc.
ATTN: G. Hesselbacher

Applied Theory, Inc.
2 cy ATTN: J. Trulio

Artec Associates, Inc.
ATTN: S. Gill

Avco Research & Systems Group
ATTN: W. Broding
ATTN: Research Lib., A830, Rm. 7201

Battelle Memorial Institute
ATTN: Technical Library
ATTN: R. Klingsmith

BDM Corp.
ATTN: A. Lavagnino
ATTN: Technical Library

BDM Corp.
Albuquerque International
ATTN: R. Hensley

Bell Telephone Laboratories
ATTN: J. White

Boeing Co.
ATTN: Aerospace Library
ATTN: R. Dyrdaahl
ATTN: R. Carlson

Brown Engineering Company, Inc.
ATTN: M. Patel

California Institute of Technology
ATTN: T. Ahrens

California Research & Technology, Inc.
ATTN: K. Kreyenhagen
ATTN: Technical Library
ATTN: S. Shuster

Calspan Corp.
ATTN: Technical Library

Center for Planning & Rsch., Inc.
ATTN: R. Shnider

Civil/Nuclear Systems Corp.
ATTN: R. Crawford

DEPARTMENT OF DEFENSE CONTRACTORS (Continued)

University of Dayton
Industrial Security Super, KL-505
ATTN: H. Swift

University of Denver
Colorado Seminary
ATTN: Sec. Officer for J. Wisotski

EG&G Washington Analytical Services Center, Inc.
ATTN: Technical Library
ATTN: Director

Electric Power Research Institute
ATTN: G. Slater

Electromechanical Sys. of New Mexico, Inc.
ATTN: R. Shunk

Engineering Decision Analysis Co., Inc.
ATTN: R. Kennedy

Franklin Institute
ATTN: Z. Zudans

Gard, Inc.
ATTN: G. Neidhardt

General Dynamics Corp.
Pomona Division
ATTN: K. Anderson

General Dynamics Corp.
Electric Boat Division
ATTN: M. Pakstys

General Electric Co.
Space Division, Valley Forge Space Center
ATTN: M. Bortner, Space Sci. Lab.

General Electric Co.
Re-Entry & Environmental Systems Div.
ATTN: A. Ross

General Electric Co.-TEMPO
Center for Advanced Studies
ATTN: DASAC

General Research Corp.
Santa Barbara Division
ATTN: B. Alexander

Geocenters, Inc.
ATTN: F. Marram

H-Tech Laboratories, Inc.
ATTN: B. Hartenbaum

Honeywell, Inc.
Defense Systems Division
ATTN: T. Helvig

IIT Research Institute
ATTN: Technical Library
ATTN: R. Welch

Northwestern University
Dept. of Civil Engineering
ATTN: T. Belytschko

DEPARTMENT OF DEFENSE CONTRACTORS (Continued)

Institute for Defense Analyses
ATTN: IDA, Librarian, R. Smith
ATTN: Director

J H Wiggins, Co., Inc.
ATTN: J. Collins

Kaman Avidyne
Division of Kaman Sciences Corp.
ATTN: N. Hobbs
ATTN: F. Criscione
ATTN: Technical Library

Kaman Sciences Corp.
ATTN: P. Ellis
ATTN: Library
ATTN: F. Shelton

Karagozian and Case
ATTN: J. Karagozian

Lockheed Missiles & Space Co., Inc.
ATTN: Technical Library

Lockheed Missiles & Space Co., Inc.
ATTN: T. Geers, D/52-33, Bldg. 205
ATTN: P. Underwood

Lovelace Foundation for Medical Education & Research
ATTN: Asst Dir. of Res., R. Jones
ATTN: Technical Library

Martin Marietta Corp.
Orlando Division
ATTN: G. Fotio

McDonnell Douglas Corp.
ATTN: R. Halprin

McMillan Science Associates, Inc.
ATTN: R. Oliver

Merritt CASES, Inc.
ATTN: Technical Library
ATTN: J. Merritt

Meteorology Research, Inc.
ATTN: W. Green

University of New Mexico
Dept. of Campus Security and Police
ATTN: G. Triandafalidis

Nathan M. Newmark
Consulting Engineering Services
ATTN: N. Newmark

Pacific Technology
ATTN: R. Bjork
ATTN: G. Kent

Physics International Co.
ATTN: F. Sauer
ATTN: C. Vincent
ATTN: R. Swift
ATTN: E. Moore
ATTN: D. Orphal
ATTN: L. Behrmann
ATTN: Technical Library

DEPARTMENT OF DEFENSE CONTRACTORS (Continued)

Prototype Development Associates, Inc.
ATTN: T. McKinley

R&D Associates

ATTN: J. Lewis
ATTN: H. Brode
ATTN: C. Knowles
ATTN: J. Carpenter
ATTN: W. Wright, Jr.
ATTN: R. Port
ATTN: A. Fields
ATTN: Technical Library
ATTN: P. Rausch
ATTN: A. Latter

Rand Corp.

ATTN: A. Laupa
ATTN: Technical Library
ATTN: C. Mow

Science Applications, Inc.
ATTN: Technical Library

Science Applications, Inc.
ATTN: S. Oston

Science Applications, Inc.
ATTN: D. Bernstein
ATTN: D. Maxwell

R&D Associates

ATTN: H. Cooper

Science Applications, Inc.
ATTN: B. Chambers
ATTN: W. Layson

Southwest Research Institute
ATTN: W. Baker
ATTN: A. Wenzel

SRI International
ATTN: G. Abrahamson

Systems, Science & Software, Inc.
ATTN: T. Riney
ATTN: Technical Library
ATTN: R. Sedgewick
ATTN: D. Grine
ATTN: T. Cherry

DEPARTMENT OF DEFENSE CONTRACTORS (Continued)

Terra Tek, Inc.
ATTN: Technical Library
ATTN: A. Jones
ATTN: S. Green

Tetra Tech, Inc.

ATTN: L. Hwang
ATTN: Technical Library

Texas A & M University System
C/O Texas A & M Research Foundation
ATTN: H. Coyle

TRW Defense & Space Sys. Group

ATTN: P. Bhutta
ATTN: N. Lipner
ATTN: D. Jortner
ATTN: Tech. Info. Center
2 cy ATTN: P. Dai

TRW Defense & Space Sys. Group

San Bernardino Operations
ATTN: G. Hulcher
ATTN: F. Wong

Universal Analytics, Inc.
ATTN: F. Field

The Eric H. Wang
Civil Engineering Rsch. Fac.
The University of New Mexico
ATTN: N. Baum
ATTN: L. Bickle

Weidlinger Assoc., Consulting Engineers

ATTN: M. Baron
ATTN: J. McCormick

Weidlinger Assoc., Consulting Engineers

ATTN: J. Isenberg

Westinghouse Electric Corp.

Marine Division
ATTN: W. Volz